Supporting Information

The facile activation of graphite for the improved determination of dopamine, acetamidophenol and rutin

Yanxue Xu[a], Guihua Chen[b], Yunting Qin[b] and Dan Xiao[a,c]*

[a]*Institute of Advanced Study, Chengdu University, No. 2025, Chengluo Avenue, Chengdu, P. R. China*

[b]*Sichuan Industrial Institute of Antibiotics, Chengdu University, No. 2025, Chengluo Avenue, Chengdu, P. R. China*

[c]*College of Chemical Engineering, Sichuan University, No. 29 Wangjiang Road, Chengdu, P. R. China*

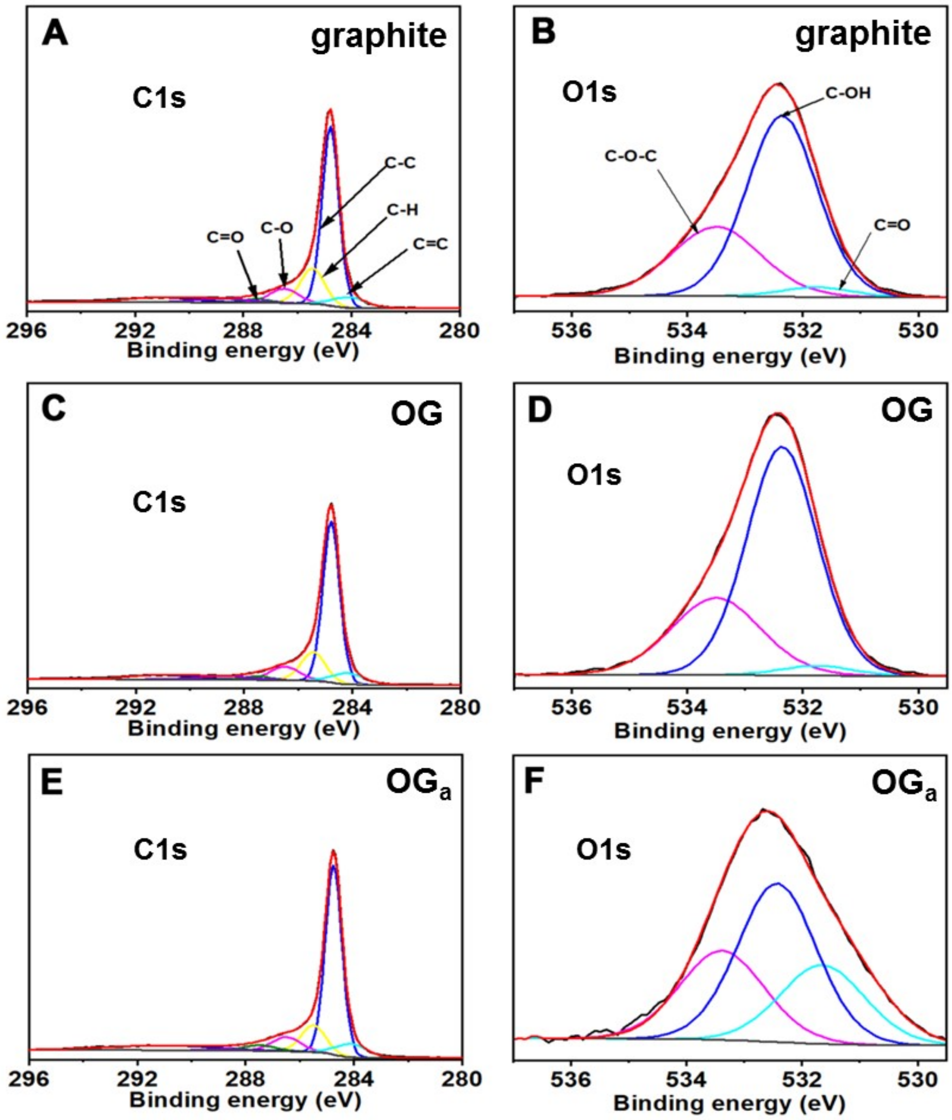

Figure S1 XPS spectrum: (A-B) the C 1s and O 1s core peaks of graphite; (C-D) the C 1s and O 1s core peaks of OG; (E-F) the C 1s and O 1s core peaks of OG_a. OG_a was OG being cycled in PBS (pH 6.0) containing the analytes of DA, RT and APAP with 100 cycles. The concentration of the analytes was 200 μM.

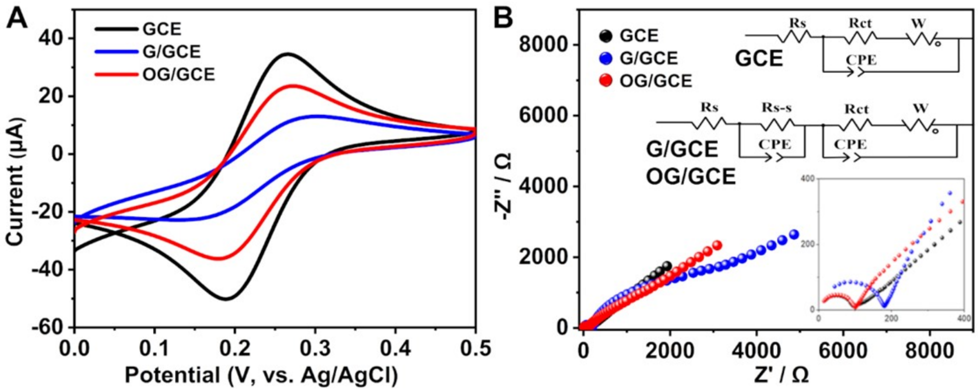

Figure S2 (A) CV curves of bare GCE, G/GCE, OG/GCE in 0.1 M KCl with 1.0 mM $[Fe(CN)_6]^{3-/4-}$ at 50 mV/s; (B) EIS of bare GCE, G/GCE, OG/GCE at a constant potential of 0.25 V in 0.1 M KCl with 1.0 mM $[Fe(CN)_6]^{3-/4-}$ and the corresponding equivalent circuit diagrams.

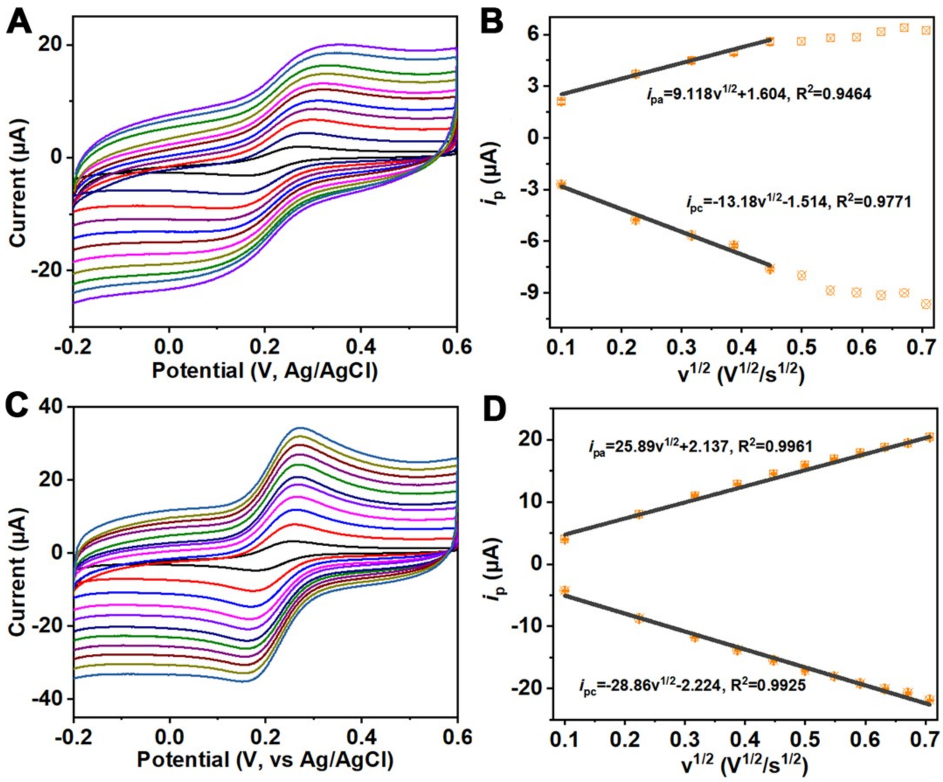

Figure S3 Cyclic voltammograms and the corresponding linear plots of i_p versus $v^{1/2}$ of G/GCE (A, B) and OG/GCE (C, D) at different scan rates: 10, 50,100, 150, 200, 250, 300, 350, 400, 450, 500 mV/s in 1.0 mM $K_3Fe(CN)_6$ containing 0.1 M KCl.

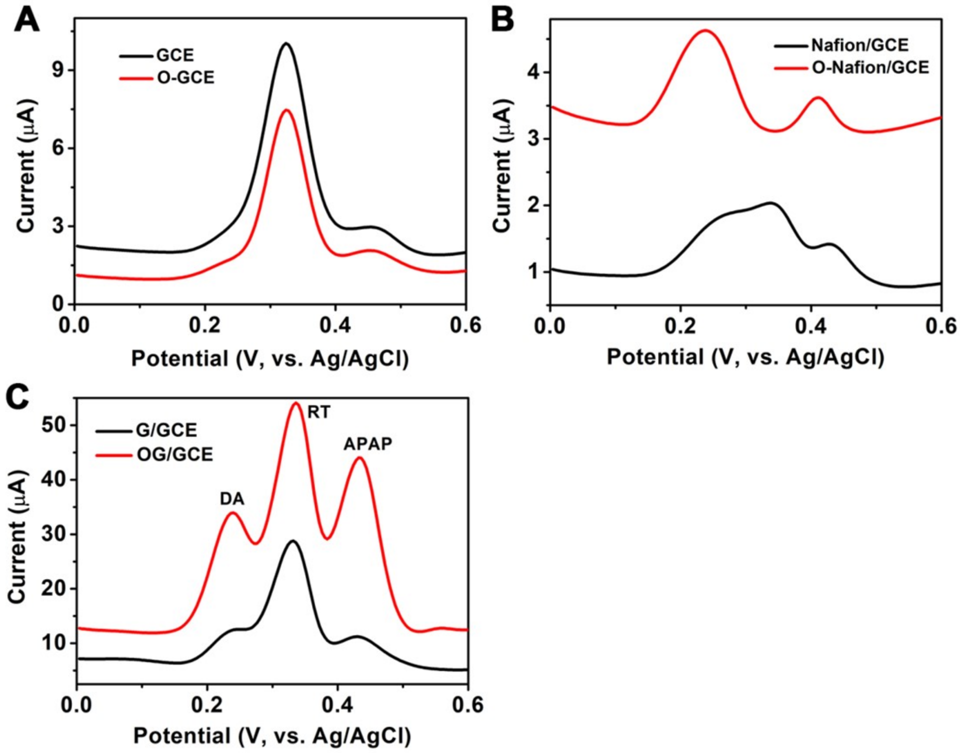

Figure S4 DPV curves of different electrodes before (black curve) and after (red curve) being immersed in sodium peroxide solution for 2 min: (A) bare GCE, (B) Nafion/GCE, (C) G/GCE. The medium is PBS (pH 6.0) with 10 μM DA, 4.0 μM RT and 50 μM APAP.

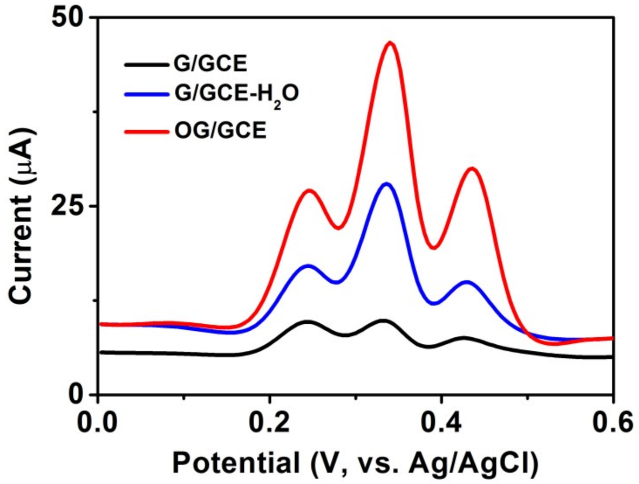

Figure S5 DPV curves of G/GCE (black curve), G/GCE immersed in water for 2 min ($G/GCE-H_2O$, blue curve) and OG/GCE (red curve) immersed in sodium peroxide solution for 2 min toward 10 μM DA, 1.0 μM RT and 30 μM APAP.

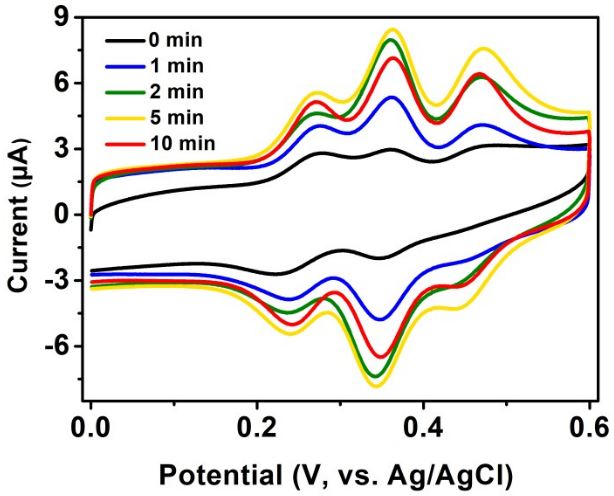

Figure S6 CV curves of OG/GCE immersed in Na_2O_2 solution for different time responding to DA, RT and APAP.

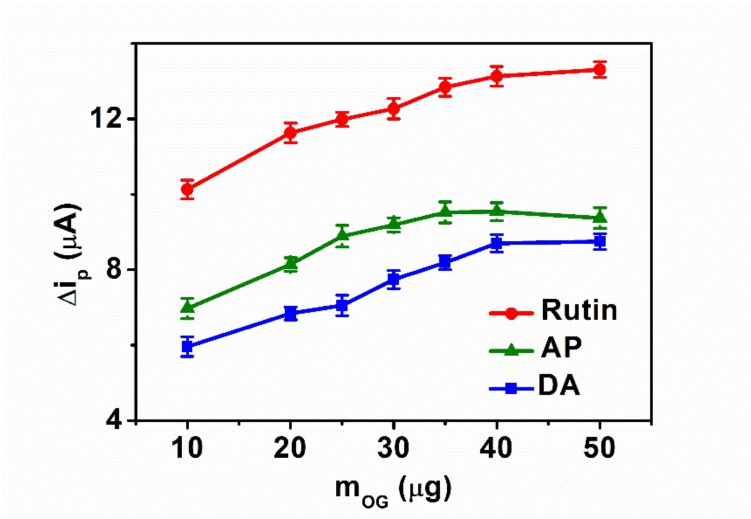

Figure S7 OG/GCE modified with different mass of graphite toward DA, RT and APAP . Error bar was calculated by three replicates.

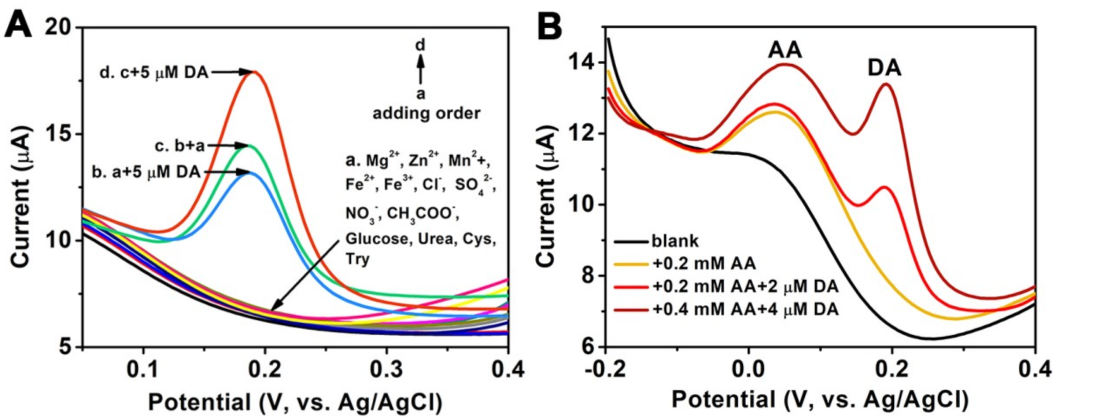

Figure S8 (A) Selectivity of OG/GCE towards DA against with the coexisting interferents, the adding order is: a. interferents (1 mM); b. first addition of 5 μM DA; c. second addition of the interferents (1 mM); d. second addition of 5 μM DA. **(**B) Interference studies of OG/GCE towards DA against with high concentration of ascorbic acid (AA).

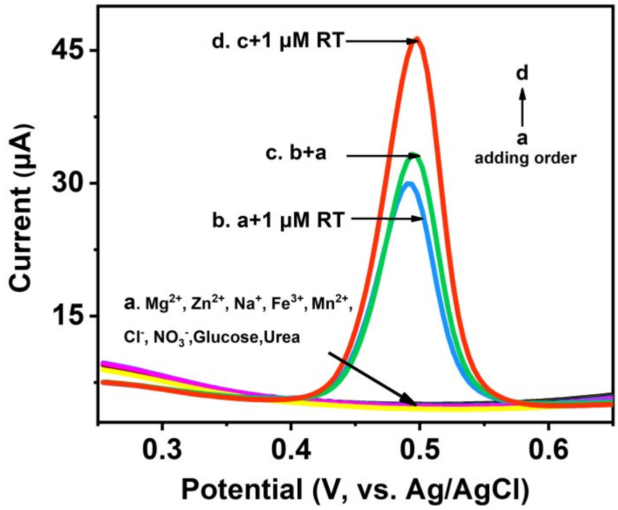

Figure S9 Selectivity of OG/GCE towards RT against with the coexisting interferents, the adding order is: a. interferents (1 mM); b. first addition of 1.0 μM RT; c. second addition of the interferents (1 mM); d. second addition of 1.0 μM RT.

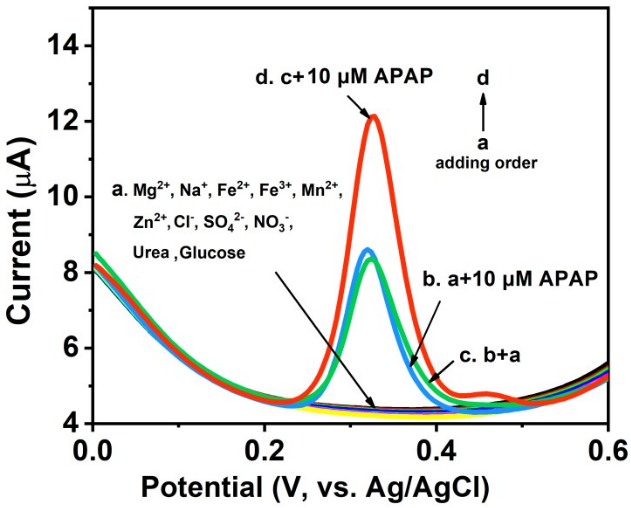

Figure S10 Selectivity of OG/GCE towards APAP against with the coexisting interferents, the adding order is: a. interferents (1 mM); b. first addition of 10 μM APAP; c. second addition of the interferents (1 mM); d. second addition of 10 μM APAP.

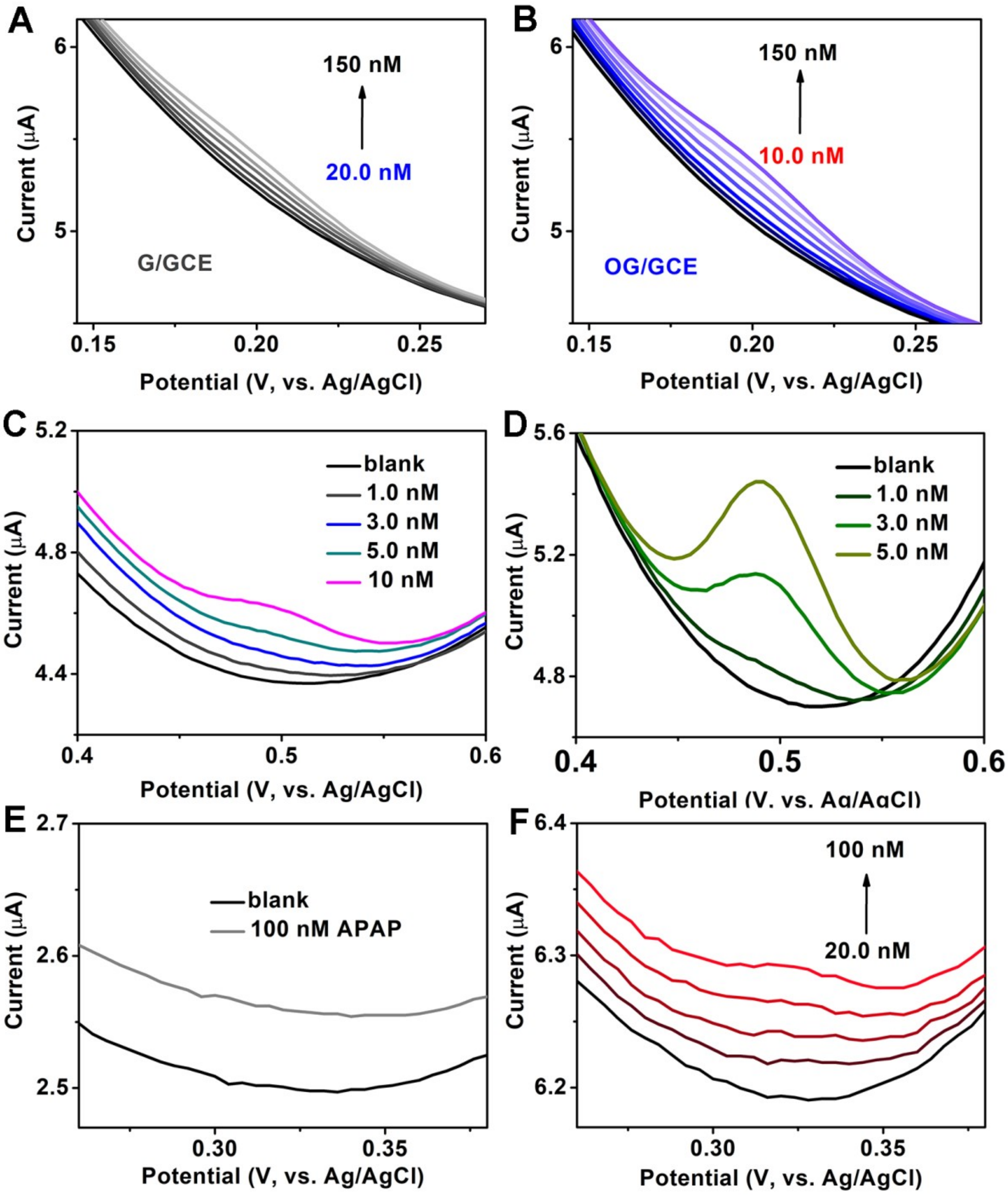

Figure S11 DPV curves about the detection limits of G/GCE (left) and OG/GCE (right) toward DA (A-B), RT (C-D) and APAP (E-F).

Table S1. OG/GCE compared with the reported sensors for the detection of DA, RT and APAP.

Electrodes	Methods	Linear range			LOD (μM)	Ref.
		RT (μM)	DA (μM)	APAP (μM)		
MXene-$FeWO_4$/GCE	SWV	0.001-0.147	--	--	0.00042	1
MIP/AuNPs-MoS_2-GN/GCE[a]	DPV	0.01-45.0	--	--	0.004	2
Mg-Al-Si@PC/GCE[b]	DPV	1-10	--	--	0.01	3
ICBG/SPCE[c]	DPV	0.08-52	--	--	0.011	4
Nafion-GO-IL/CILE[d]	DPV	0.08-100	--	--	0.016	5
PEDOT-MC/AgNPs/GCE[e]	DPV	0.005-0.5	--	--	0.0035	6
Ru-(L-Ala)-C_3N_4/GCE	DPV	--	0.06-490	--	0.02	7
NC/MWCNT/GCE[f]	DPV	--	1-200	--	0.6	8
AgPd@Zr-MOF/GCE	SWV	--	2-42	--	0.1	9
AuNPs/N-doped CN/SPE[g]	DPV	--	0.02-700	--	0.007	10
Ag/CuO/ITO	CV	--	0.04-10	--	0.007	11
Fe/Fe_3N@carbon nanocomposite	DPV	--	0.05-66.4	0.05-56.9	0.97/0.21	12
phosphorus-doped graphene/GCE	DPV	--	--	1.5-120	0.36	13
Fc-rGO/PMo_{12}/GCE[h]	DPV	--	--	1-1000	0.013	14
Pd-MWCNTs/GCE	DPV	--	--	0.5-100	0.13	15
Ni/C-400/GCE[i]	DPV	--	--	0.20-53.75	0.0404	16
Pt/NGr/GCE[j]	SWV	--	--	0.05-90	0.008	17
OG/GCE	DPV	0.010-10	0.001-0.15	0.020-30	0.0062 0.00036 0.013	This Work

a. molecularly imprinted polymer/ Au nanoparticles-MoS_2-graphene

b. porous carbon encapsulated Mg-Al-Si alloy

c. indium-doped copper bismuthate/graphene

d. Nafion/graphene oxide/ionic liquid/ carbon ionic liquid electrode

e. poly(3,4-ethylene-dioxythiophene)/mesoporous carbon/Ag nanoparticles

f. nickel cobaltite/multi-walled carbon nanotube

g. Au nanoparticles/N-doped carbon nanorods

h. ferrocene based reduced graphene oxide/PMo_{12}

i. nickel-doping nanoporous carbon

j. platinum nitrogen-doped graphene nanocomposite

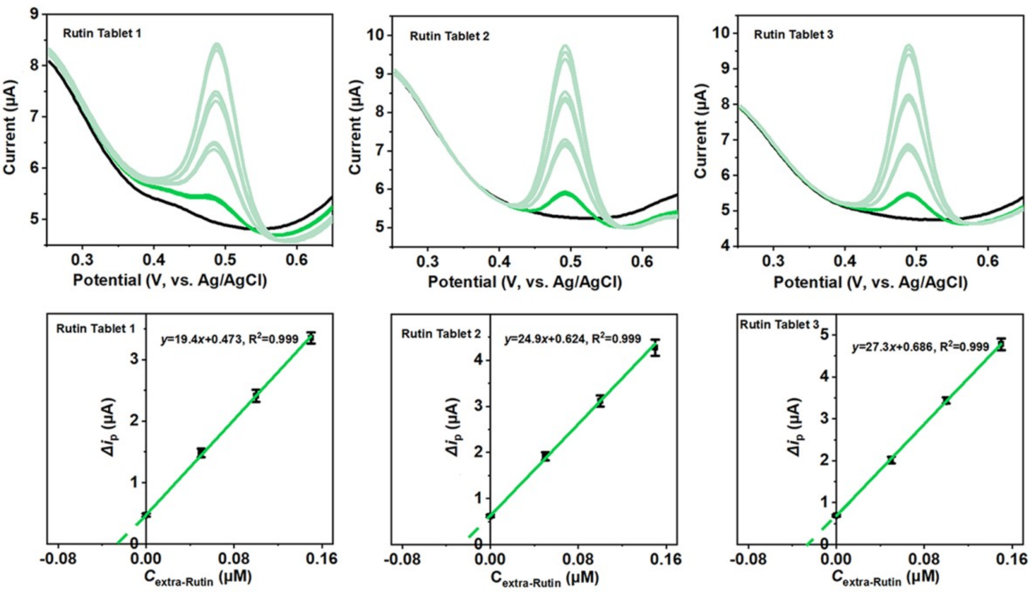

Figure S12 Determination of RT in three rutin tablets: DPV curves and the corresponding linear fitting plots of Δi_p-C_{RT}. The labelled content of RT is 20 mg/tablet.

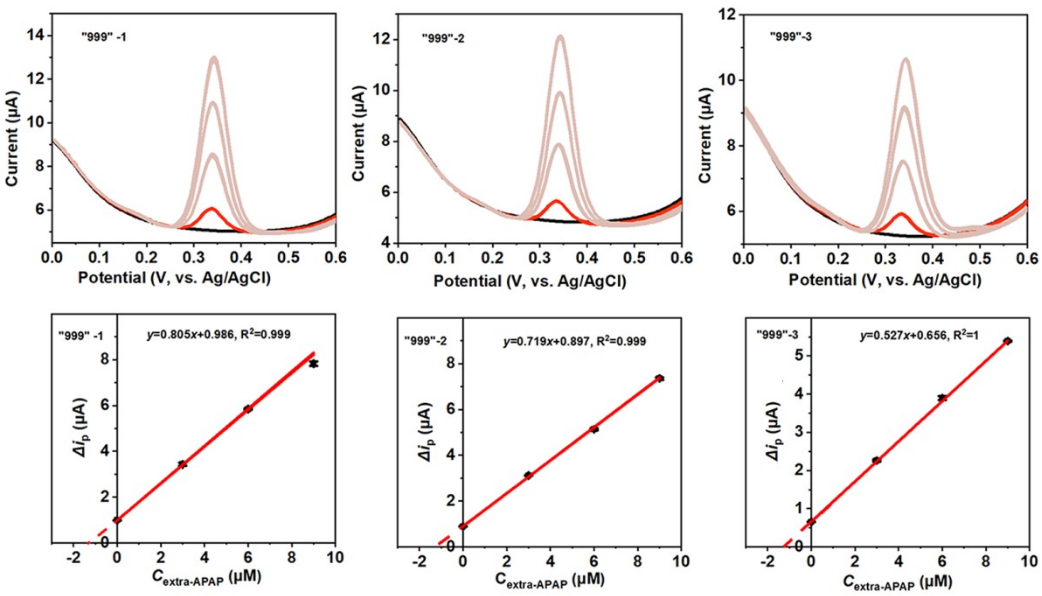

Figure S13 Determination of APAP in three bags of 999 Ganmaoling granules: DPV curves and the corresponding linear fitting plots of Δi_p-C_{APAP}. The labelled content of APAP is 200 mg/10 g.

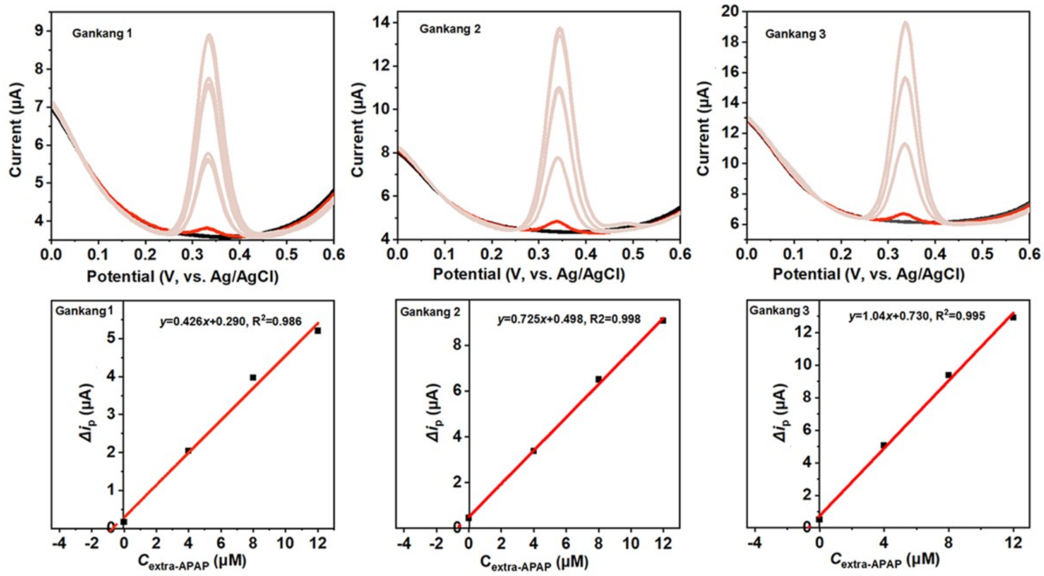

Figure S14 Determination of APAP in three Gankang tablets: DPV curves and the corresponding linear fitting plots of Δi_p-C_{APAP}. The labelled content of APAP is 250 mg/tablet.

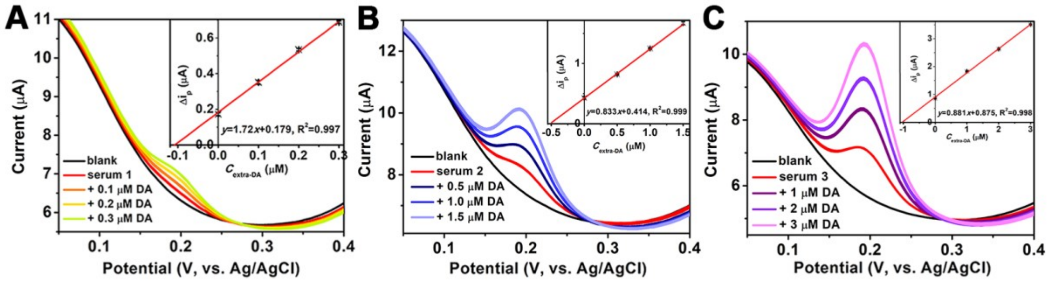

Figure S15 Recovery experiments of DA in serums from 3 people: (A-C) DPV curves and the corresponding linear fitting plots. The working electrode was OG/GCE.

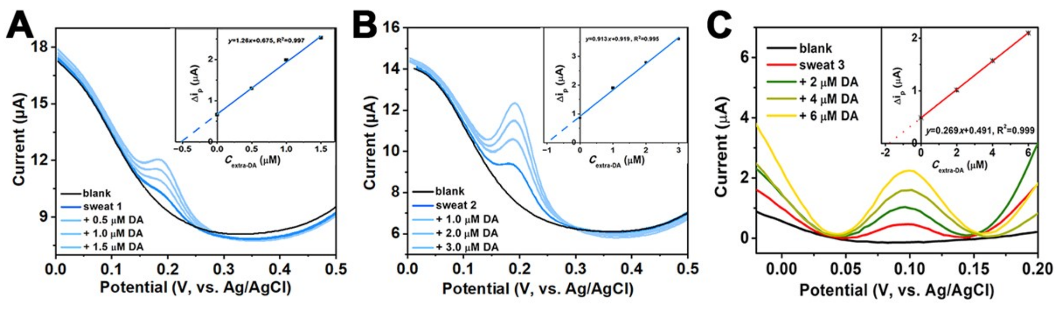

Figure S16 Recovery experiments of DA in sweats from 3 people: (A-C) DPV curves and the corresponding linear fitting plots. Sweat 1 and sweat 2 were detected by

OG/GCE, sweat 3 was detected by OG/SPCE.

Reference

1. Ranjith K. S., Vilian A. T. E., Ghoreishian S. M., Umapathi R., Huh Y. S., Han Y. K., *Sensor Actuat. B Chem.*, 2021, **344**, 130202.
2. Wang Y., Zhang B., Tang Y., Zhao F., Zeng B., *Microchem. J.*, 2021, **168**, 106505.
3. Yalikun N., Mamat X., Li Y., Hu X., Wang P., Hu G., *Microchim. Acta*, 2019, **186**, 379.
4. Kaleeswarran P., Koventhan C., Chen S.-M., Arumugam A., *Colloid. Surface. A*, 2022, **643**, 128740.
5. Hu S., Zhu H., Liu S., Xiang J., Sun W., Zhang L., *Microchim. Acta*, 2012, **178**, 211-219.
6. Zhang B., Jaouhari A. E., Wu X., Liu W., Zhu J., Liu X., *J. Electroanal. Chem.*, 2020, **877**, 114632.
7. Xie X., Wang D. P., Guo C., Liu Y., Rao Q., Lou F., Li Q., Dong Y., Li Q., Yang H. B., Hu F. X., *Anal. Chem.*, 2021, **93**, 4916-4923.
8. Poolakkandy R. R., Neelakandan A. R., Puthiyaparambath M. F., Krishnamurthy R. G., Chatanathodi R., Menamparambath M. M., *J. Mater. Chem. C*, 2022, **10**, 3048-3060.
9. Hira S. A., Nagappan S., Annas D., Kumar Y. A., Park K. H., *Electrochem. Commun.*, 2021, **125**, 107012.

10. Shi Z., Wu X., Zou Z., Yu L., Hu F., Li Y., Guo C., Li C. M., *Biosens. Bioelectron.*, 2021, **186**, 113303.

11. Li Y. Y., Kang P., Wang S. Q., Liu Z. G., Li Y. X., Guo Z., *Sensor Actuat. B Chem.*, 2021, **327**, 128878.

12. Cai X. Q., Huang Y., Luo Y. H., Liu Y., Zhang Q. Y., Zhao Z. A., Zhu Q., Chen F. Y., Zhang D. E., *Solid State Sci.*, 2022, **132**, 106984.

13. Zhang X., Wang K. P., Zhang L. N., Zhang Y. C., Shen L., *Anal. Chim. Acta*, 2018, **1036**, 26-32.

14. Han H., Liu C., Sha J., Wang Y., Dong C., Li M., Jiao T., *Talanta*, 2021, **235**, 122751.

15. Wu Y., Wu Y., Lv X., Lei W., Ding Y., Chen C., Lv J., Feng S., Chen S.-M., Hao Q., *Mater. Chem. Phys.*, 2020, **239**, 121977.

16. Guo L., Hao L., Zhang Y., Yang X., Wang Q., Wang Z., Wang C., *Talanta*, 2021, **228**, 122228.

17. Anuar N. S., Basirun W. J., Ladan M., Shalauddin M., Mehmood M. S., *Sensor Actuat. B Chem.*, 2018, **266**, 375-383.